

Healing kinetics of interfacial voids in GaAs wafer bonding

YewChung Sermon Wu and Guo-Zen Hu

Citation: [Applied Physics Letters](#) **81**, 1429 (2002); doi: 10.1063/1.1502194

View online: <http://dx.doi.org/10.1063/1.1502194>

View Table of Contents: <http://scitation.aip.org/content/aip/journal/apl/81/8?ver=pdfcov>

Published by the [AIP Publishing](#)

Articles you may be interested in

[Nanoscaled interfacial oxide layers of bonded n - and p -type GaAs wafers](#)

Appl. Phys. Lett. **88**, 172104 (2006); 10.1063/1.2198511

[Kinetic study of thermally induced electronic and morphological transitions of a wafer-bonded GaAs/GaAs interface](#)

J. Appl. Phys. **94**, 2423 (2003); 10.1063/1.1592293

[High-temperature healing of interfacial voids in GaAs wafer bonding](#)

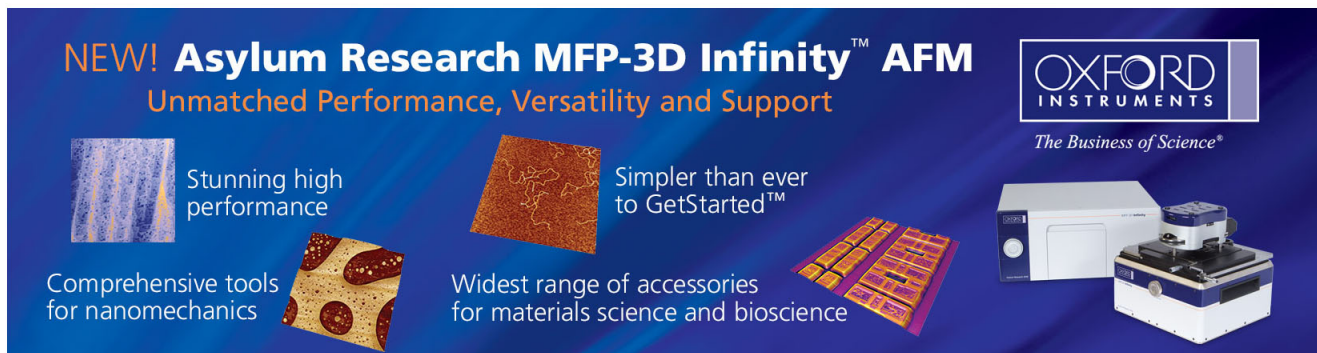
J. Appl. Phys. **91**, 1973 (2002); 10.1063/1.1430888

[Chemical investigations of GaAs wafer bonded interfaces](#)

J. Appl. Phys. **90**, 5991 (2001); 10.1063/1.1416139

[Interface structures in GaAs wafer bonding: Application to compliant substrates](#)

Appl. Phys. Lett. **76**, 2674 (2000); 10.1063/1.126440

The advertisement features a dark blue background with white and orange text. At the top left, it says 'NEW! Asylum Research MFP-3D Infinity™ AFM' in large white letters, followed by 'Unmatched Performance, Versatility and Support' in orange. On the right, the 'OXFORD INSTRUMENTS' logo is shown in white, with the tagline 'The Business of Science®' below it. The central part of the ad contains four images with descriptive text: 1) A blue textured surface with the text 'Stunning high performance'. 2) A brown textured surface with the text 'Simpler than ever to GetStarted™'. 3) A yellow and red patterned surface with the text 'Comprehensive tools for nanomechanics'. 4) A white and blue AFM instrument with the text 'Widest range of accessories for materials science and bioscience'. The Oxford Instruments logo and tagline are positioned to the right of the central text.

Healing kinetics of interfacial voids in GaAs wafer bonding

YewChung Sermon Wu^{a)} and Guo-Zen Hu

Department of Materials Science and Engineering, National Chiao Tung University, Hsinchu 300, Taiwan

(Received 1 May 2002; accepted for publication 28 June 2002)

A periodic structure of bonded GaAs wafers has been proposed for quasi-phase-matched second-harmonic generation. After bonding, voids were formed at the interface due to the natural topographical irregularities and contamination on the wafer surface. Within the voids, crystallites with diamond-shaped and dendritic geometries were found, which corresponded to the bonded regions. In this study, artificial voids were introduced at the bonded interface to study the growth kinetics of these crystallites, that is the healing kinetics of these voids. It was found that the crystallite geometries and the growth rates are controlled by the nucleation of new surface layers on the bonded planes, which was the slowest stage during the healing process. © 2002 American Institute of Physics. [DOI: 10.1063/1.1502194]

Bonding of III–V semiconductors was originally developed for two-layer optoelectronic devices.^{1–4} Bonding processes were usually performed at elevated temperatures to increase the bonding strength and bonded area.^{5,6} The bonding temperature could be decreased to as low as 150 °C, if the wafers were cleaned with atomic hydrogen, and then bonded inside an UHV apparatus.^{3,7} However, regardless of the bonding temperature, voids were always found at the interface. These voids were caused by natural topographical irregularities, surface contamination, solvent residues, trapped gases, and/or misorientation between the wafers.

Based on the studies mentioned above, a periodic structure of bonded GaAs wafers was proposed for quasi-phase-matched (QPM) second-harmonic generation (SHG).^{5,6,8} In this structure, each layer had to be rotated 180° from the adjacent one. This in turn created a twin boundary at the interface. After bonding, voids were also found at the interface. Infrared transmission microscopy revealed two kinds of bonding features (crystallites) in these voids: diamond/rhombohedral geometry and dendrite geometry.⁵

Similar crystallites were found in studies of crack-healing in ceramic materials.^{9,10} Four stages have been identified in the ceramic crack-healing process: (a) a continuous regression of the void from the void tip or a discontinuous pinch-off of the void along the lengths of the voids, (b) cylinderization of the voids, (c) breakup of the cylindrical voids into rows of isolated pores, and (d) shrinkage or growth of isolated pores. The morphological changes and transport mechanisms in crack healing were found to bear significant similarities to those in the GaAs wafer bonding processes. As a result, the research findings in crack healing were applied in the studies of the interfacial voids in GaAs wafer bonding.

In our previous studies,^{5,6} artificial voids were introduced at the interface to investigate the first healing stage of interfacial voids in GaAs wafer bonding. It involved the creation of controlled voids in one wafer surface by etching it with photolithographically generated patterns, and then bonding it to an unpatterned wafer. Using this approach, we

were able to vary the void shape (disks, squares, and rectangles), size (ranging from 5–500 μm) and depth (ranging from 10 to 3000 nm), and therefore simulate the interfacial defects caused by natural topographical irregularities on the wafer surface.

After high temperature bonding (850–950 °C), regardless of the void geometry, most crystallites formed in the voids were initiated (nucleated) by the mechanism of pinch-off along the lengths of the voids. This pinch-off phenomenon did not change even when various compressive stresses (0–3 MPa) were applied during bonding.^{5,6}

At the twin boundary, the growth of crystallites had two principal morphologies: a dendrite geometry and a diamond/rhombohedral geometry, as shown in Fig. 1. These two different features resulted from surface energy anisotropy and/or growth rate anisotropy.^{5,6} When the void depth h was ≥ 200 nm, by the Gibbs–Thomson calculation, the driving force for growth was small. The shapes of crystallites were resulted mainly from surface energy anisotropy.⁵ Most of the crystallites were diamond-shaped, as shown in Fig. 1(a). The

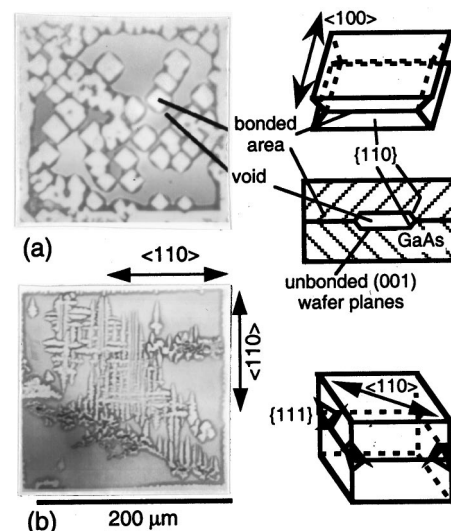


FIG. 1. IR transmission optical micrograph of artificial voids at (001) GaAs twin boundary: (a) $h = 200$ nm, 900 °C, 10 h and (b) $h = 70$ nm, 900 °C, 4 h.

^{a)} Author to whom correspondence should be addressed; electronic mail: sermonwu@stanfordalumni.org

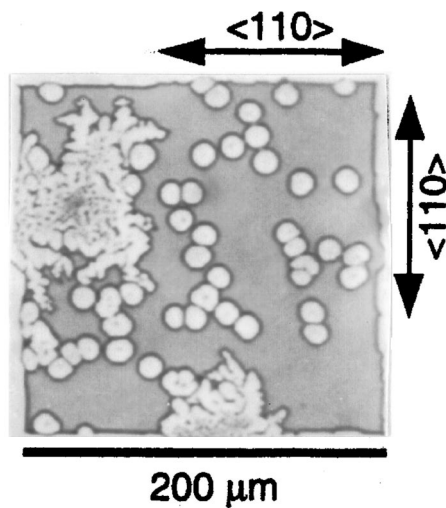


FIG. 2. IR transmission optical micrograph of 70 nm deep artificial voids at (001) GaAs normal boundary bonded at 900 °C for 8 h.

edges of the diamond features were elongated in the $\langle 100 \rangle$ direction, which was bounded by low surface energy $\{110\}$ planes. On the other hand, when the void depth was small ($h \leq 70$ nm), the driving force was larger. According to the growth rate anisotropy, as shown in Fig. 1(b), dendrites grew quickly in the $\langle 110 \rangle$ direction, which was bounded by fast growing $\{111\}$ planes.⁵

The growth kinetics of these interfacial crystallites, however, was still not clear. Therefore, in this study, the growth kinetics of these crystallites (the healing kinetics of interfacial voids) was investigated by bonding two GaAs wafers with their crystallographic axes aligned relative to one another. The boundary between these two bonded wafers were designated as “normal boundary.”

After bonding, the majority of the crystallites formed at the normal boundary were in the shape of cylinder (Fig. 2). Most of these cylinder crystallites were nucleated by the pinch-off mechanism, regardless of bonding temperature (850–950 °C), void geometry, or compressive stress. It was also found that the growth rates of cylinders were much slower than that of dendrites and diamonds.

As shown in Fig. 3, there are three stages related to the growth rates of these crystallites during the bonding process: (1) decomposition from unbonded (001) wafer planes, (2) mass transport, and (3) deposition on the exposed bonded planes. Since the crystallite geometries and the growth rates

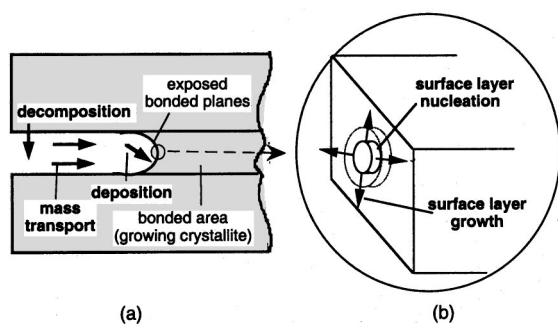


FIG. 3. (a) Three stages related to the growth of the bonded areas (crystallites): decomposition, mass transport, and deposition (b) Two steps related to the deposition stage: surface layer nucleation and surface layer growth.

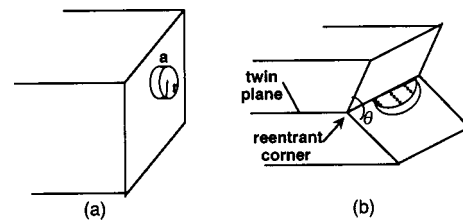


FIG. 4. Schematic illustration of the primary layer source mechanism involved in crystallite growth: (a) two-dimensional pillbox nucleation and (b) twin-plane reentrant corner.

are controlled by the slowest stage above, it is crucial to identify the slowest stage. If either decomposition or mass transport was the slowest stage during the bonding process, the observed crystallite geometries and the growth rates of both twin and normal boundaries should be very similar. This is due to the fact that the major difference between these two boundaries is that the twin boundary has an artificial (001) twin at the bonded interface, while the normal boundary does not. They are not much different in their unbonded wafer planes and mass transport paths. However, this hypothesis was not supported by observation. For instance, most of the crystallites formed at the twin boundary were in the shapes of dendrite (for $h \leq 70$ nm) or diamond (for $h \geq 200$ nm), but most of the crystallites formed at the normal boundary were cylinder shaped (regardless of the void depth). Moreover, the growth rates of dendrites and diamonds were 10 times higher than that of cylinders. These observations clearly eliminated decomposition and mass transport as the slowest stage. Therefore, the slowest stage should be the deposition on the exposed bonded planes.

Furthermore, as shown in Fig. 3, there are two limiting steps in the deposition stage: (1) surface layer nucleation and (2) surface layer growth. If the layer growth was the slower limiting step, the crystallite geometries and the growth rates of both twin and normal boundaries should be similar. However, as mentioned previously, the crystallites formed at these two boundaries were quite different. On the other hand, if the layer nucleation was the slower limiting step, each nucleation event should result in the crystallization of an entire layer, thus the surface of exposed bonded planes should be very smooth. This smooth surface has been verified by a previous transmission electron microscope analysis.⁵ The above observations clearly demonstrated that layer growth is not the slower step. At the same time, it suggested that surface layer nucleation is more likely to be the slower limiting step of crystallite growth in bonded areas.

The nucleation rate of a new surface layer depended on the boundary of bonded GaAs wafers. For a normal boundary, new layers were uniformly distributed on the crystallite surface, which can be described by a pillbox model.¹¹ With respect to the formation of a pillbox-shaped island [Fig. 4(a)], the energy barrier is given by

$$\Delta G^{\text{dep}}(r) = (-\pi r^2 a) \Delta G_i + 2\pi r a \gamma_\ell,$$

where r is the island radius, a is the lattice distance, ΔG_i is the deposition driving force, and γ_ℓ is the ledge free energy.

There will be a maximum in $\Delta G^{\text{dep}}(r)$ at some $r = r^*$.

This maximum will act as an effective energy barrier to the formation of a new pillbox-shaped island. The maximum can

be found by setting $\Delta G^{\text{dep}'} = 0$. We find $r^* = \gamma_\ell / \Delta G_i$ and $\Delta G^{\text{dep}'}(r^*) = \pi a \gamma_\ell^2 / \Delta G_i$. For the nucleation of pillbox-shaped layers, the crystallite growth rate is given by

$$V = aAI = aAI_0 \exp[-\Delta G^{\text{dep}'} / kT] \\ = aAI_0 \exp[-\pi a \gamma_\ell^2 / (kT \Delta G_i)], \quad (1)$$

where A is the area available for nucleation of new layer, I is the nucleation frequency per unit area, and T is the temperature. In Eq. (1), it is assumed that the layer growth rate is infinitely rapid compared to the formation rate of new pillboxes. Therefore, each nucleation event results in the crystallization of an entire layer. If this does not hold, then the Eq. (1) needs to be multiplied by a factor < 1 .¹¹

As for a (001) twin plane, layers were produced by the nucleation on the reentrant corners in Fig. 4(b).¹¹ In this case, the critical radius and effective energy barrier of formation of the half-box island are given by

$$r_{\text{tw}}^* = \frac{\gamma}{\Delta G_i}, \quad \Delta G_{\text{tw}}^{\text{dep}'}(r_{\text{tw}}^*) = 0.5 \pi a \gamma^2 / \Delta G_i,$$

and

$$\gamma = \gamma_\ell + \frac{2}{\pi} [\gamma_{\text{tw}} - \Delta \gamma(\phi)],$$

where γ_{tw} is the twin boundary energy and $\Delta \gamma(\phi)$ is the change in the surface energy of the flat edge, which is in contact with the adjacent tilted face.¹¹ This calculation shows that the formation energy of a partial pillbox island is lower than that of a full pillbox island. Therefore, according to Eq. (1), the crystallite growth rate at the twin boundary was much higher than that at the normal boundary. In other words, the growth rates of diamonds and dendrites were much higher than that of cylinders.

Artificial voids, which were used to simulate gaps formed between GaAs wafers during bonding, were introduced at the bonded interface to study the healing kinetics of

voids. It was found that crystallites formed within these artificial voids during the bonding process and corresponded to the bonded regions within the voids. Their geometries and growth rates were controlled by the nucleation of new layers on the bonded planes. When there was a normal boundary at the bonded interface, the nucleation of a new layer on the bonded planes could be described by a pillbox model. Most of the crystallites were in the shape of cylinder and their growth rates were slow. On the other hand, when there was a (001) twin boundary at the interface, the twin-plane reentrant corners lowered the formation energy for the partial pillbox island. Therefore, most of the crystallites were in the shapes of dendrite or diamond with much higher growth rates than that of cylinder crystallites.

This project was funded by National Science Council (NSC) of the Republic of China under Grant No. NSC90-2216-E009-037, and has benefited from the facilities and equipment of Semiconductor Research Center at National Chiao Tung University.

¹F. A. Kish, D. A. Vanderwater, M. J. Peanasky, M. L. Ludowise, S. G. Hummel, and S. J. Rosner, *Appl. Phys. Lett.* **67**, 2060 (1995).

²Z. L. Liao and D. E. Mull, *Appl. Phys. Lett.* **56**, 737 (1990).

³T. Akatsu, A. Plöbs, H. Stenzel, and U. Gösele, *J. Appl. Phys.* **86**, 7146 (1999).

⁴F. A. Kish, D. A. Vanderwater, M. J. Peanasky, M. J. Ludowise, S. G. Hummel, and S. J. Rosner, *Appl. Phys. Lett.* **67**, 2060 (1995).

⁵Y. S. Wu, P. C. Liu, R. S. Feigelson, and R. K. Route, *J. Appl. Phys.* **91**, 1973 (2002).

⁶Y. S. Wu, R. S. Feigelson, R. K. Route, D. Zheng, L. A. Gordon, M. M. Fejer, and R. Byer, *J. Electrochem. Soc.* **145**, 366 (1998).

⁷G. Kastner, T. Akatsu, St. Senz, A. Plöbs, and U. Gösele, *Appl. Phys. A: Mater. Sci. Process.* **70**, 13 (2000).

⁸L. A. Gordon, G. L. Woods, R. C. Eckardt, R. K. Route, R. S. Feigelson, M. M. Fejer, and R. Byer, *Electron. Lett.* **29**, 1942 (1993).

⁹T. K. Gupta, *Structure and Properties of MgO and Al₂O₃ Ceramics* (American Ceramic Society, Columbus, OH, 1984), p. 750.

¹⁰Z. Wang, Y. Z. Li, M. P. Harmer, and Y. T. Chou, *J. Am. Ceram. Soc.* **75**, 1596 (1992).

¹¹W. A. Tiller, *The Science of Crystallization Microscopic Interfacial Phenomena* (Cambridge University Press, Cambridge, 1991), p. 76.